트렐리스 부호화된 MDPSK-OFDM의 다중 위상차 검파

김 종 일
관동대학교 정보기술공학부

Multiple Phase Differential Detection of Trellis-coded MDPSK-OFDM

Chong-Il Kim
Devision of Information Technologies Eng., Kwandong University

Abstract

In this paper, the Viterbi decoder containing new branch metrics of the squared Euclidean distance with multiple order phase differences is introduced in order to improve the bit error rate (BER) in the differential detection of the trellis-coded MDPSK-OFDM. The proposed Viterbi decoder is conceptually same as the multiple phase differential detection method that uses the branch metric with multiple phase differences. Also, we describe the Viterbi algorithm in order to use this branch metrics. Our study shows that such a Viterbi decoder improves BER performance without sacrificing bandwidth and power efficiency. Also, the proposed algorithm can be used in the single carrier modulation.

I. Introduction

For mobile radio communication systems, the demands of multimedia communications are increasing to provide a variety of high-quality multimedia services. This requires the high-bandwidth efficiency and high data rate transmission systems. Multicarrier modulation schemes, often called orthogonal frequency-division multiplexing (OFDM), is one of the techniques which meet such requirements with reasonable complexity.

In this paper, the Viterbi decoder with branch metrics of the squared Euclidean distance of the first up to the multiple phase differences is introduced in order to improve the BER performance in differential detection of TC MDPSK. Exploitation of branch metrics is thus well integrated in our detailed Viterbi algorithm. Then we investigate the performance of the TC 8DPSK-OFDM in an additive white Gaussian noise (AWGN), Rician and Rayleigh fading channels. Our study shows that the MDPSK with trellis-code i.e., TC MDPSK-OFDM, is an attractive scheme for power and bandlimited systems. Especially, the Viterbi decoder with multiple phase difference metrics improves the BER performance. Although this investigation is made for an OFDM transmission system, the proposed method to perform multiple phase differential detection (MPDD) is not limited to OFDM. The metric proposed for TC 8DPSK-OFDM can be used for single-carrier transmission systems as well.

II. Transmission System and TC MDPSK-OFDM

Fig. 1 shows the considered TC MDPSK-OFDM transmission system. And the Fig. 2 shows the set partition by the phase difference at the $\pi/4$ shift QPSK.

Consider a transmitted signal over the OFDM symbol k

$$u_k^n = \frac{1}{\sqrt{MC}} \sum_{i=0}^{MC-1} U_k^i \, e^{j2\pi ni/MC} \quad (1)$$

where U_k^i is the TC MDPSK symbol in the ith subcarrier at the kth symbol and MC is the number of subcarriers. U_k^i has the following complex form

$$U_k^i = \exp(j\theta_k^i) \quad (2)$$

where θ_k^i denotes the transmitted signal phase and takes one of the M values from the set $\{2\pi m/M, m=0,1,\cdots,M-1\}$.

III. MPDD of Trellis-coded MDPSK-OFDM

1. Trellis Decoding of TC MDPSK-OFDM with MPDD

In this paper, we will show that the Viterbi decoder can improve the BER performance by using the branch metric with first up to the Lth order phase differences although the trellis branch has only one symbol. The Viterbi decoder is equivalent to the multiple phase differential detection (MPDD) by means of using the branch metric with multiple phase differences. The multiple symbol differential scheme uses two first-order phase differences and one second-order phase difference among three symbols. As shown in Fig.3, this process uses only one multiple phase difference per 3 signals.

But, the MPDD which is proposed in our paper uses the consecutive multiple phase difference in spite of having the one phase difference symbol on the trellis branch. As shown in Fig.3, whenever one channel signal is inputted, one first order phase difference symbol and one second order phase difference symbol are calculated. So, we call this scheme as MPDD because it looks like a sliding window fashion.

The lth order phase difference at subcarrier i in the received $(l+1)$ adjacent OFDM symbols, $g^{i,a}_{l,k}$ can be derived as

$$\begin{aligned} g^{i,a}_{l,k} &= V^i_k \cdot V^{i\,*}_{k-l} \\ &\approx |\alpha^i_k|^2 \cdot f_k \cdot f_{k-1} \cdots f_{k-l+1} \\ &\quad + \alpha^i_k \cdot U^i_k \cdot N^{i\,*}_{k-l} + \alpha^{i\,*}_k \cdot U^{i\,*}_{k-l} \cdot N^i_k \end{aligned} \tag{3}$$

Let $g^i_{l,k}$ be

$$\begin{aligned} g^i_{l,k} &\equiv \frac{g^{i,a}_{l,k}}{|\alpha^i_k|^2} = f_k \cdot f_{k-1} \cdots f_{k-l+1} \\ &\quad + \frac{1}{\alpha^{i\,*}_k \cdot U^{i\,*}_k} \cdot N^{i\,*}_{k-l} \\ &\quad + \frac{1}{\alpha^i_k \cdot U^i_{k-l}} \cdot N^i_k \\ &= f_k \cdot f_{k-1} \cdots f_{k-l+1} + N^i_{l,k} \end{aligned} \tag{4}$$

and the pdf of $g^i_{l,k}$ can be expressed as

$$\begin{aligned} &P_G(g^i_{l,k} \mid f_k, f_{k-1}, \cdots, f_{k-l+1}) \\ &\approx \frac{1}{\sigma_{l,k}\sqrt{2\pi}} \exp\left\{ \frac{-(g^i_{l,k} - f_k \cdot f_{k-1} \cdots f_{k-l+1})^2}{2\sigma^2_{l,k}} \right\} \end{aligned} \tag{5}$$

If we use L continuous phase differences, then

$$P_G(G|\hat{F}) = \max_{all\ F} \prod_{k=L}^{N-1} P(g^i_{1,k}, \cdots g^i_{L,k} \mid f_k \cdots f_{k-L+1}) \tag{6}$$

Generally, it is computationally easier to use the logarithm of the likelihood-function since this permits the summation rather than the multiplication of terms. We assume that the noise random variables are jointly Gaussian distributed and the channel is memoryless. They are also mutually independent. Therefore the conditional pdf of the channel differential signal becomes

$$\begin{aligned} \ln P_G(G|\hat{F}) = \max_{all\ F} \ln \prod_{k=L}^{N-1} \frac{\left|[C_{G^i_k G^i_k}]^{-1}\right|^{1/2}}{(2\pi)^{L/2}} \\ \times \exp\left\{ -\frac{[G^i_k - \overline{G^i_k}]^H [C_{G^i_k G^i_k}]^{-1} [G^i_k - \overline{G^i_k}]}{2} \right\} \end{aligned} \tag{7}$$

where $[C_{G^i_k G^i_k}]$ is the covariance matrix of a block of extracted phase differences.

Then

$$\begin{aligned} \ln P_G(G|\hat{F}) = \max_{all\ F} \Big[K - \sum_{k=L}^{N-1} A [G^i_k - \overline{G^i_k}]^H \\ \cdot [C_{G^i_k G^i_k}]^{-1} [G^i_k - \overline{G^i_k}] \Big] \end{aligned} \tag{8}$$

where A and K are constants that can be disregarded in the maximization. In conclusion, the maximum-likelihood detector based on a sequence of signal G^i_k seeks F which minimizes the following path metric

$$\begin{aligned} \lambda_p = \min_{all\ F} \Big[\sum_{k=L}^{N-1} [G^i_k - \overline{G^i_k}]^H \\ \cdot [C_{G^i_k G^i_k}]^{-1} [G^i_k - \overline{G^i_k}] \Big] \end{aligned} \tag{9}$$

We define the branch metric of the Viterbi decoder of the TC MDPSK-OFDM demodulation as the following:

$$\lambda_b = [G^i_k - \overline{G^i_k}]^H [C_{G^i_k G^i_k}]^{-1} [G^i_k - \overline{G^i_k}] \tag{10}$$

If we use L continuous phase differences, the suboptimal branch metric finally becomes

$$\begin{aligned}\lambda_b &= |g^i_{1,k} - f^i_k|^2 + |g^i_{2,k} - f^i_k \cdot f^i_{k-1}|^2 + \cdots \\ &\quad + |g^i_{L,k} - f^i_k \cdot f^i_{k-1} \cdots f^i_{k-L+1}|^2 \\ &= |V^i_k \cdot V^{i\,*}_{k-1} - f^i_k|^2 \\ &\quad + |V^i_k \cdot V^{i\,*}_{k-2} - f^i_k \cdot f^i_{k-1}|^2 + \cdots \\ &\quad + |V^i_k \cdot V^{i\,*}_{k-L} - f^i_k \cdot f^i_{k-1} \cdots f^i_{k-L+1}|^2\end{aligned} \tag{11}$$

A demodulation block diagram of the TC MDPSK-OFDM with MPDD is shown in Fig. 4.

2 Viterbi Decoding Algorithm with MPDD

We will demonstrate how to construct a Viterbi decoder with the above metric. In this case, the decisions depend on not only the Euclidean distance of the present phase difference signal but also on the Euclidean distances of previous L-1 phase difference signals. In order to compute other terms, let

$c^f_k(m,n)$:candidate signal between the state m at $t=k$ and the state n at $t=k+1$ where $m,n=0,1,\cdots,S-1$, S is a state number;

$c^b_{k-j\cdot MC}(m,n)$:candidate signal of the survivor path between the state m at $t=k-j\cdot MC$ and the state n at $t=k-j\cdot MC+1$ where $m,n=0,1,\cdots,S-1$, $j=L-1,L-2,\cdots,1$ and S is a state number.

Then, $c^f_k(0,0)$ is the signal number 0 and $c^f_k(0,1)$ is the signal number 2 at Fig. 2. The f^i_{k-1} is the phase difference signal of subcarrier i in the previous OFDM symbol $k-1$. Therefore this is same to the branch signal between $t=k-MC$ and $t=k-MC+1$ of the trellis diagram.

The algorithm can be described as the following:

step 1 : Find the candidate signal $c^f_k(m,n)$ for all the state at time $t=k$

step 2 : Find the candidate signal $c^b_{k-j\cdot MC}(m,n)$ between the states at $t=k-j\cdot MC$ and the state at $t=k-j\cdot MC+1$ by backward searching the survivor path, where $j=L-1,L-2,\cdots,1$.

step 3 : In order to calculate $|g^i_{L,k} - f^i_k \cdot f^i_{k-1} \cdot f^i_{k-L+1}|^2$ of eq. (11), calculate $c^f_k(m,n) \cdot c^b_{k-MC}(m,n) \cdots c^f_{k-L\cdot MC+1}(m,n)$.

step 4 : Calculate the branch metric using eq. (11).

step 5 : Repeat step 4 for the number of branch per state.

step 6 : Repeat step 1,2,3,4 for the number of state.

step 7 : Update and compare the path metric at $t=k+1$ and find the survivor path at $t=k+1$.

step 8 : Decode the information data.

Here, L is smaller than the decoding delay of the Viterbi decoder.

For example, as shown in Fig. 5, consider L=2 and state number equals 2.

Ⅳ.Numerical Examples

The performance improvement of the TC 8DPSK-OFDM over the uncoded DQPSK-OFDM is investigated based on the Monte Carlo method. OFDM systems with 256 subcarriers are simulated respectively. Interleaving is performed by a block interleaver with 16×16 for each subcarrier number. A guard interval ($=MC/4$) is added to the discrete time signal as a periodic extension of the IFFT output sequence. It is assumed that the transmitted signal is corrupted by the AWGN, Rician or Rayleigh channel.

Ⅴ. Conclusions

The proposed Viterbi decoder is based on a multiple phase differential detection method that uses the branch metric with the first up to the Lth order phase differences. Also, we describe the Viterbi algorithm in order to use such branch metrics.

Through this method, a performance improvement of 3.5-4.3 dB at a 10^{-5} BER is obtained over the uncoded DQPSK-OFDM for AWGN. We also reveal the fact that the BER performance for Rician channel can be improved up to 4.4-5.6 dB. For Rayleigh channel, the uncoded OFDM and 4 or 8-state TC 8DPSK-OFDM with or without MPDD yield the error floor. But for the 16-state TC 8DPSK-OFDM, error floor doesn't occur and the performance increases to 1.6 dB with the MPDD. These improvements are achieved without sacrificing any bandwidth efficiency (data rate) or power efficiency.

Reference

[1] S. Hara and R. Prasad, Overview of multicarrier CDMA, *IEEE Commun. Mag.*, no. 9, pp. 126-133, Dec. 1997.

[2] G. Ungerboeck, Channel coding with multilevel phase signals, *IEEE Trans. Inf. Theory*, vol. IT-28, pp. 55-67, Jan. 1982.

[3] D. Divsalar and M. K. Simon, Multiple trellis-coded modulation (MTCM), *IEEE Trans. Commun.*, vol. COM-36, no. 4, pp. 410-419, Apr. 1988.
[4] S. Samejima, K. Enomoto, and Y. Watanabe, Differential PSK system with nonredundant error correction, IEEE Journal on Selected Areas in Communications, vol. SAC-1, no. 1, pp. 74-81, Jan. 1983.
[5] D. Divsalar and M. K. Simon, Multiple-symbol differential detection of MPSK, *IEEE Trans. Commun.*, vol. COM-38, no. 3, pp. 300-308, Mar. 1990.
[6] D. Divsalar and M. K. Simon, and M. Shahshahani, The performance of trellis-coded MPSK with multiple symbol detection, *IEEE Trans. Commun.*, vol. COM-38, no. 9, pp. 1391-1403, Sept. 1990.
[7] T. May, H. Rohling and V. Engels, Performance Analysis of Viterbi Decoding for 64-DAPSK and 64-QAM modulated OFDM Signals, *IEEE Trans. Commun.*, vol. 46, no. 2, pp. 182-190, Feb. 1998.

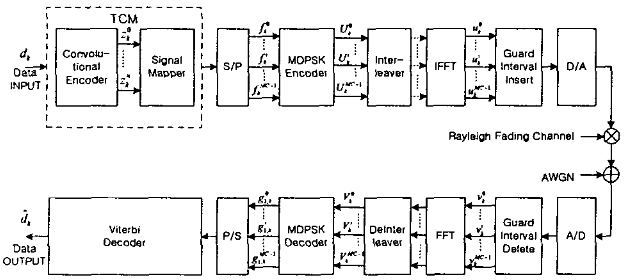

Fig. 1. TC MDPSK-OFDM Transmission System.

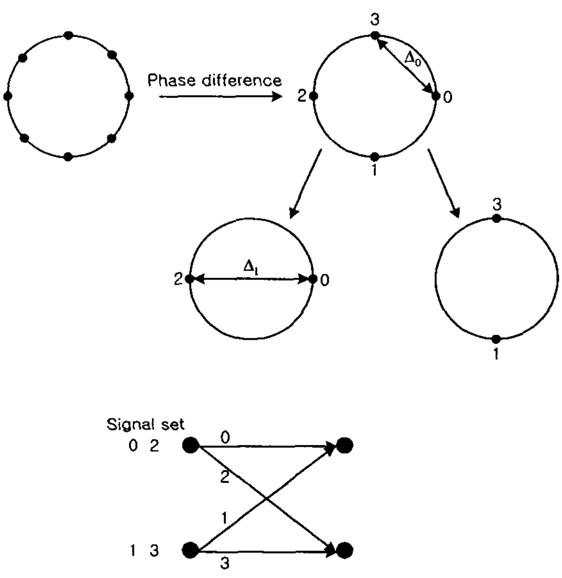

Fig. 2. The set partition and trellis diagram by the phase difference at the $\pi/4$ shift QPSK.

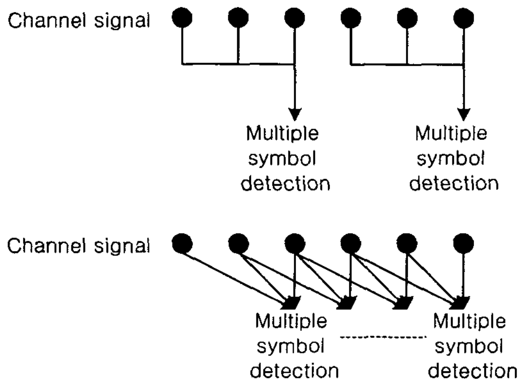

Fig. 3. Comparison of the conventional multiple symbol detection and the MPDD

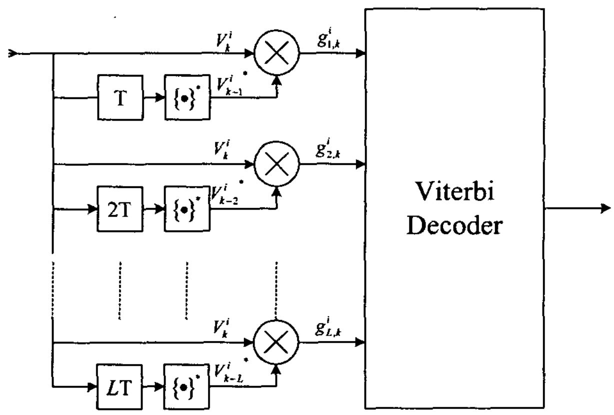

Fig. 4. Demodulation block diagram of TC MDPSK-OFDM with the Lth phase difference of ith subcarrier.

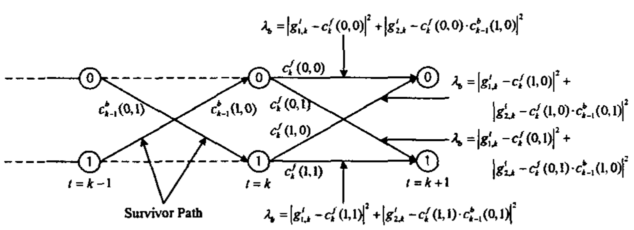

Fig. 5. Trellis diagram of the Viterbi decoder with the Lth difference metric ($L=2$)

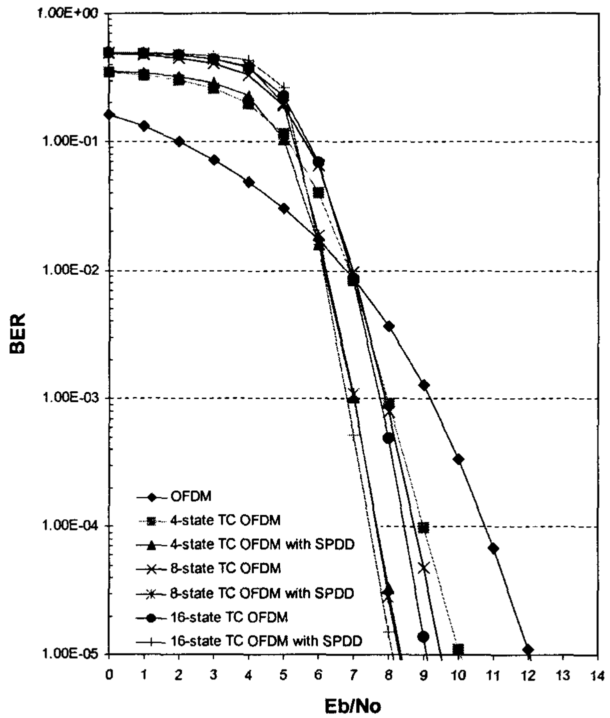

Fig. 6. Performance of the OFDM and the TC 8DPSK-OFDM with MPDD for AWGN channel (subcarrier number=256).

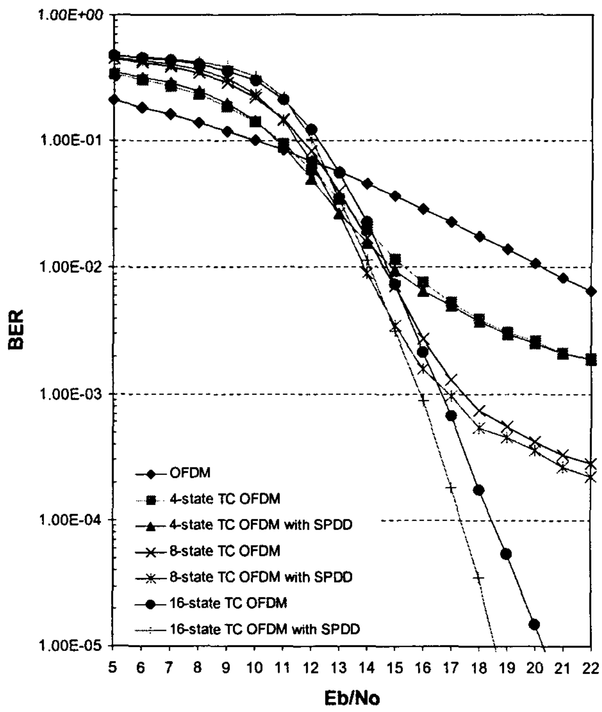

Fig. 8. Performance of the OFDM and the TC 8DPSK-OFDM with SPDD for Rayleigh channel (subcarrier number=256).

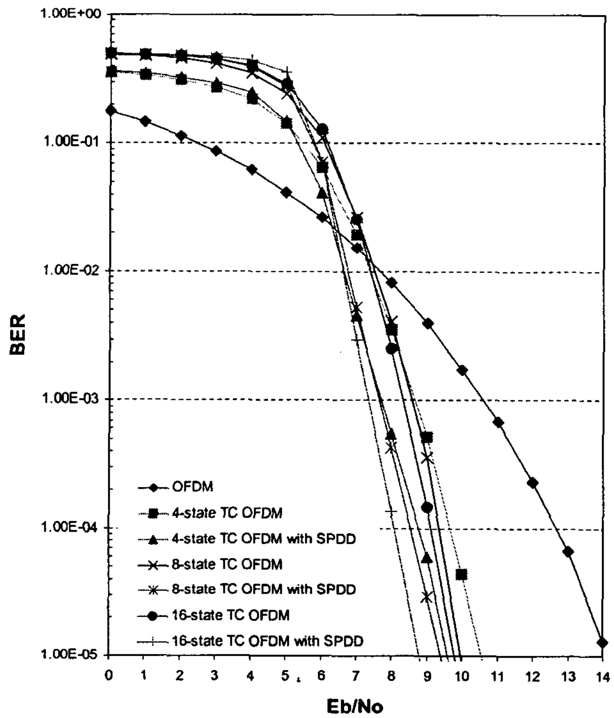

Fig. 7. Performance of the OFDM and the TC 8DPSK-OFDM with SPDD for Rician channel (subcarrier number=256)